Hindawi
Journal of Nanomaterials
Volume 2021, Article ID 5530606, 9 pages
https://doi.org/10.1155/2021/5530606

Research Article

Comparing Thermal Durability and Effects of Annealing Temperature on Characteristics of Hydrogen-Doped ZnO, AZO, and GZO Thin Films

Dung Van Hoang,[1,2] **Anh Tuan Thanh Pham**,[1,2] **Truong Huu Nguyen**,[1,2] **Thang Bach Phan**,[1,2,3] **and Vinh Cao Tran**[1,2]

[1]*Laboratory of Advanced Materials, University of Science, HoChiMinh City, Vietnam*
[2]*Vietnam National University, HoChiMinh City, Vietnam*
[3]*Center for Innovative Materials and Architectures, HoChiMinh City, Vietnam*

Correspondence should be addressed to Vinh Cao Tran; tcvinh@hcmus.edu.vn

Received 17 January 2021; Revised 14 February 2021; Accepted 28 February 2021; Published 18 March 2021

Academic Editor: Duong Tuan Quang

In this work, undoped, aluminum-, and gallium-doped ZnO thin films (ZnO-H, AZO-H, and GZO-H, respectively) deposited on soda-lime glass substrates by magnetron sputtering method in a gas mixture of hydrogen and argon are annealed at various temperatures in the range of 200–500°C in air to evaluate the durability of those films under annealing temperature. From photoluminescence spectra, formation of point defects, especially oxygen vacancies, when hydrogen diffuses out of the films at high annealing temperature is exhibited via a significant increase of visible emissions. We find out that carrier concentration and Hall mobility of AZO-H and ZnO-H films dramatically decrease, while those of GZO-H film are still stable as the annealing temperature increased from 200°C to 300°C. We proposed a model for interpreting the thermal durability of GZO-H film that, at an annealing temperature of 300°C, Ga^{3+} ions located at adjacent Zn sites can push hydrogen atoms, which are broken out of the antibonding sites which are perpendicular to the $\boldsymbol{c}$ -axis (AB⊥), into bond center sites paralleled to the $\boldsymbol{c}$ -axis ($BC_{//}$). The movement of hydrogen from AB⊥ to $BC_{//}$ site also gives rise to the durability of electrical properties of GZO-H films at the high annealing temperature.

1. Introduction

ZnO, a native n-type oxide semiconductor, owning a wide bandgap (3.37 eV) along with a high exciton energy of 60 meV, has been extensively investigated in recent years due to its ability for UV detectors, photoelectric electronic devices, or thin film solar cells [1, 2]. However, efficiency of those devices is strongly affected by intrinsic or extrinsic defects, which are generated during depositing, such as zinc interstitials (Zn_i), oxygen vacancies (V_O), or zinc vacancies (V_{Zn}) [1–3]. Therefore, the intrinsic or extrinsic defects are popularly investigated by researchers via simulations or experiments to depress and enhance the useless and useful defects, respectively.

Zn_i and V_O play role as donors in ZnO material [3–5]. Ghose et al. [4] proved that Zn_i and V_O can exist in different charged states. For example, the yellow emission from photoluminescence spectra is attributed to doubly charged oxygen vacancies ($V_O^{\bullet\bullet}$) ($^{\bullet}$ is the Kröger–Vink notation) or the blue luminescence is attributed to Zn_i. Lin et al. [5] also proved that Zn_i and V_O still exist in ZnO films regardless of growing in high oxygen partial pressure. Huang et al. [6] theoretically proved the migration barrier of Zn_i that has a very small value, about 0.3–0.5 eV, which could mobile down to very low temperature. Besides, those authors also showed that V_{Zn} is stable at room temperature. Apart from mentioned intrinsic defects, the un- or intentional extrinsic defects, especially defects related to hydrogen, also play a crucial role

on characteristics of ZnO thin films. Van de Walle exploded the researches related to hydrogen in ZnO [7] after the conclusion that hydrogen behaves as a shallow donor in ZnO thin films. After that, there have been numerous experimental as well as theoretical reports which proved and expanded the role of hydrogen in ZnO [8–16]. Hydrogen could be un- or intentionally incorporated into ZnO films during depositing and it could locate at H_{BC} or H_{AB} as the configuration proposed by Van de Walle [7]. Besides, hydrogen can also passivate defects like oxygen vacancy (V_O) or zinc vacancy (V_{Zn}) to create V_O-H (H_O) or V_{Zn}-H complex, respectively [9, 17–19], which improve electron mobility in ZnO thin films. However, hydrogen can easily diffuse out of ZnO thin films at low temperature, which leads to decreased electrical properties of ZnO thin films. Among those hydrogen-related defects, H_O may be the best thermal stable defect up to 475°C before diffusing out, while H_i (H_{BC}, H_{AB}) would diffuse out if the temperature is higher than 225°C [20]. Therefore, finding the method to improve or maintain the electrical properties of hydrogen and/or dopants codoped ZnO thin films under high temperature conditions is very important to widen applications of ZnO materials. Thus, this study investigates the effects of annealing temperature on durability of un-, aluminum-, or gallium-doped ZnO thin films and compares the thermal durability between them.

2. Experimental Details

2.1. Specimen Preparation. ZnO, AZO, and GZO thin films were deposited on soda-lime glass substrates by a dc magnetron sputtering on a Univex-450 system. All films were deposited in Ar-H gas from 3-inch ceramic un-, aluminum- (0.25 wt.% Al_2O_3), or gallium- (0.25 wt.% Ga_2O_3) doped ZnO targets. Prior to the deposition, the glass substrates were cleaned in dilute sodium hydroxide 1%, acetone, and distilled water by ultrasonic wave for 15 minutes at each step before plasma cleaning for 15 minutes. The vacuum chamber was evacuated to the base pressure of 6×10^{-6} Torr. The Ar-H gas was introduced into the sputtering chamber to reach the working pressure of 5×10^{-3} Torr. The hydrogen partial pressure ratio was calculated as the following expression: H_2 ratio = $pH_2/(pH_2 + pAr)$, where pH_2 and pAr are hydrogen and argon gas partial pressure, respectively. In this work, we prepared three series of ZnO-H, AZO-H, and GZO-H thin films at H_2 ratio of 1.7% and the substrate temperature of 200°C. The distance between the substrate and the target and sputtering power was fixed at 50 mm and 60 W, respectively. All films were annealed in air with temperature range of 200–500°C.

2.2. Characterizations. Hall effect measurement using the Van der Pauw method at room temperature on Ecopia HMS-3000 system was employed to investigate the electrical properties of the films. The transmission spectra of the films in the wavelength range of 300–1100 nm were obtained from a Jasco-730 UV-visible spectrophotometer. Film thickness was determined by using Dektak 6M surface profilometer. The film thickness of all films was maintained at 800 nm. The crystalline structure of the films was identified by X-ray diffraction (XRD) using CuKα radiation of Bruker D8 Advance system. The photoluminescence spectra obtained from NanoLog™ spectrofluorometer (Horiba) system by using the excitation wavelengths of 325 nm (He-Cd laser) were used to determinate the effects of annealing temperature on defects in ZnO thin films.

3. Results and Discussions

The dependence of carrier concentration (n) and electron mobility (μ) as a function of annealing temperature is illustrated in Figure 1. In Figure 1(a), for as-deposited films, n values of AZO-H and GZO-H films are higher than those of ZnO-H film, which indicates that group III elements effectively substituted for Zn atoms in ZnO lattice. The μ values for all films without undergoing annealing process are quite high in comparison with published reports for the similar materials and technique [21, 22]. Besides, in Figure 1(b), hydrogen shows the ability to improve the electron mobility for unannealed AZO-H and ZnO-H films better than unannealed GZO-H films. There are numerous experimental as well as theoretical publications reported that hydrogen not only behaves as a shallow donor, which gives rise to the increase of carrier concentration [8, 14, 23–28], but also passivates defects [29–31] such as V_O, Zn_i, or V_{Zn} in ZnO thin films.

The carrier concentration and electron mobility just insignificantly decrease for all films annealed at 200°C, which means that hydrogen-related defect complexes are not influenced at anneal temperature ≤ 200°C. With further increase of annealing temperature up to 300°C, there is a difference between ZnO-H and AZO-H films and GZO-H film in μ as seen in Figure 1(b). The μ values of ZnO-H and AZO-H films sharply drop from *ca.* 55 cm^2/Vs at 200°C to 2 cm^2/Vs and 12 cm^2/Vs at 300°C, respectively. The significant decrease of μ in ZnO-H and AZO-H films originates from the diffusion of hydrogen out of defect complexes, which gives rise to the formation of "dangling bond" type defects, as in silicon materials, inside the crystal grains or at the grain boundaries [8, 32, 33]. As mentioned above, H_i plays role as a shallow donor, therefore the diffusion of H_i out of crystal grains triggers reduction of carrier concentration in ZnO-H and AZO-H films. In addition, the n curves of ZnO-H and AZO-H films being similar to each other with the increase of annealing temperature (≤300°C) indicate that aluminum dopant has no roles in thermal resistance like gallium in ZnO materials as discussed below. Interestingly, n and μ of GZO-H film are not only still stable at annealing temperature of 300°C but also have a slight increasing trend. This implies that hydrogen and gallium interacted with each other in a certain way to keep stable the electrical properties of GZO-H film at 300°C. However, if the annealing temperature is higher than 400°C, n as well as μ has a dramatic decrease for all films, which indicates that hydrogen completely diffuses out of the host lattice, even H_O defects, and results in a large amount of defect.

XRD patterns, crystallite size, and full width at half maximum (FWHM) of ZnO-H, AZO-H, and GZO-H films as a function of annealing temperature are shown in Figure 2.

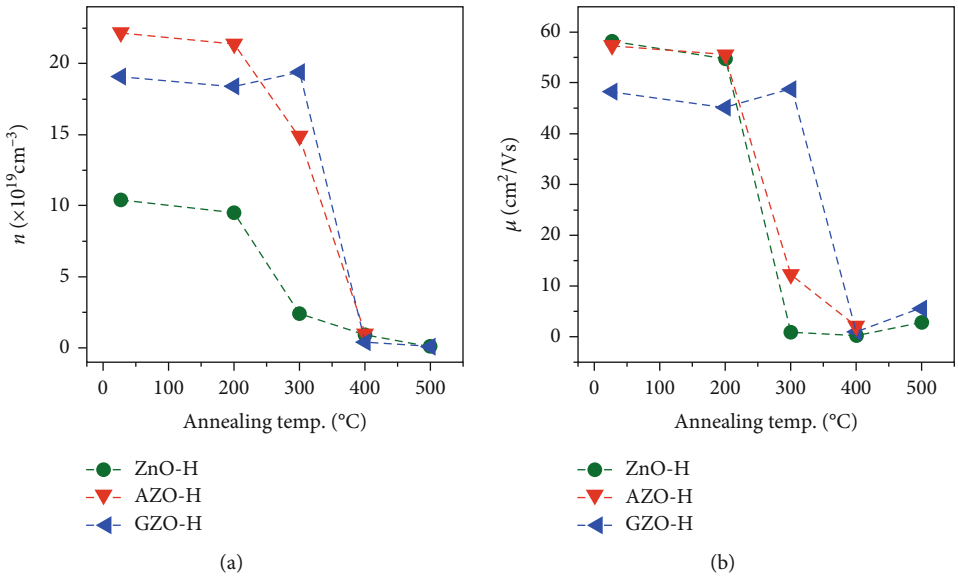

Figure 1: The variation of (a) carrier concentration and (b) electron mobility at different annealing temperatures of ZnO-H, AZO-H, and GZO-H films.

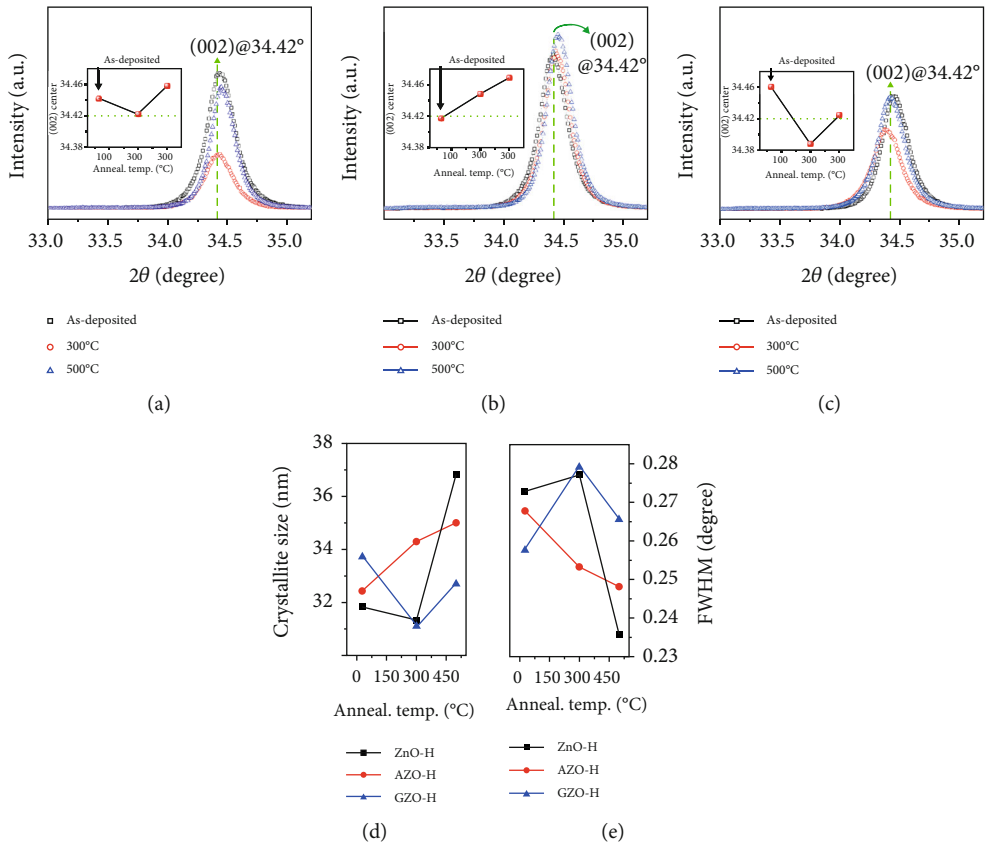

Figure 2: XRD patterns of (a) ZnO-H, (b) AZO-H, and (c) GZO-H films at different annealing temperatures. The dependence of (d) crystallite size and (e) full width at half maximum (FWHM) of ZnO-H, AZO-H, and GZO-H films on annealing temperature.

At the first glance, all films reveal a strong preferred orientation of (002) peak (JCPDS #36-1451) and the intensity of ZnO-H and GZO-H has a decrease trend, while the intensity of AZO-H films is almost unchanged as rising annealing temperature up to 300°C, which implies that there has a variation in crystal structure of these films. The recrystallisation phenomenon is observed for all films annealed at 500°C, which interprets the increase of electron mobility for all films

after being annealed at 500°C except AZO-H film which cannot be measured by Hall measurement at this temperature.

To shed light on effects of annealing temperature on the crystal structure of films, the (002) peak centers obtained from fitting these peaks based on Pearson VII function are plotted in the insets of Figures 2(a)–2(c). For ZnO-H, AZO-H, and GZO-H films without annealing treatment, the (002) peak center of AZO-H film is nearest the 2θ value of 34.42° in comparison with ZnO-H and GZO-H films, which indicates that hydrogen effectively bonds with host lattice in AZO-H film rather than in ZnO-H and GZO-H films (especially located at $BC_{//}$ site [34]) which gives rise to the significant restoration of crystal lattice and also the highest carrier concentration of AZO-H film as seen in Figure 1. However, at annealing temperature of 300°C, there has a significant decrease in the (002) peak center of ZnO-H and GZO-H films, while AZO-H film has an increase trend. Based on Bragg's equation

$$n \cdot \lambda = 2.\cdot d_{002} \cdot \sin\theta, \tag{1}$$

where n is a positive integer, λ is the wavelength of X-ray source ($\lambda_{CuK\alpha} = 0.154$ nm), and d_{002} is the interplaner spacing of the (002) plane of ZnO crystal, we reveal that the (002) peak center of ZnO-H and GZO-H films annealed at 300°C shifts towards lower 2θ angle, which means that the lattice parameter c ($c = 2d_{002}$ for hexagonal wurtzite structure of ZnO) would increase. To interpret the increase of lattice parameter c of ZnO-H and GZO-H films, we proposed some causes for this:

(1) Hydrogen atoms originated from the broken bonds of H_{AB} defects due to high temperature may move into the position between Zn-O bonds parallel c -axis. Wardle et al. [16] proved by first-principle study that the movement of hydrogen between $H_{AB\perp}$ and $H_{BC//}$ sites has relatively low barrier and they found that $H_{BC//}$ was the lowest energy structure. In addition, $H_{BC//}$ does gives rise to the increase of lattice parameter c

(2) The zinc or gallium interstitials (Zn_i or Ga_i) move into the zinc vacancies' sites (V_{Zn}—a type of electron trapping defect) which gives rise to crystal lattice restoration

(3) Oxygen interstitial (O_i) atoms move into the oxygen vacancies' sites (the existence of O_i atoms in films because of all films annealed in air ambiance). However, there is no trace of this defect in photoluminescence spectrum (discussion below) of films with annealing temperature under 300°C. Therefore, this cause may be ruled out

At annealing temperature of 300°C, the H_{AB} bonds are easy to be broken and hydrogen diffuses out of the host lattice in case of ZnO-H and AZO-H films; however, in case of GZO-H film, hydrogen is seemingly pushed by adjacent Ga^{3+} ions at Zn^{2+} site and move into the bond-center position ($H_{AB//}$). Therefore, the cause (1) interprets for the increase of the lattice parameter c, while n and μ values of GZO-H film are still stable, because H_{BC} is also considered as a shallow donor [11] and Ga_{Zn}-O-Zn-$H_{BC//}$-O complex results in the increase of lattice parameter c. The cause (2) accounts for the increase of lattice parameter c of ZnO-H film annealed at 300°C. Figure 3 is outlined to illustrate causes increasing lattice parameter c of ZnO-H and GZO-H films as elevating annealing temperature up to 300°C. However, in case of AZO-H film, the lattice parameter c monotonically decreases with further increase of annealing temperature up to 500°C, because of the hydrogen diffusion out of bond-center positions along with the small ionic radii of Al^{3+} ion ($R_{Al^{3+}} = 54$ pm) in comparison with ionic radii of Ga^{3+} ion ($R_{Ga^{3+}} = 62$ pm) and Zn^{2+} ions ($R_{Zn^{2+}} = 72$ pm) [35].

At annealing temperature of 500°C, all films have a trend of increasing lattice parameter c, because most of hydrogen in films, especially hydrogen at bond-center positions paralleled to the c-axis ($H_{BC//}$), completely diffuse out of the host lattice. Besides, Figure 2(d) shows that the crystallite size of all samples fluctuates around the value of 31–37 nm and has a slight increasing trend at high annealing temperature due to the recrystallisation phenomenon. In addition, with this large crystallite size of all films, the contribution of the boundary scattering on electrical resistivity could be omitted [36]. In addition, Figure 2(e) shows FWHM values of ZnO-H, AZO-H, and GZO-H films at various annealing temperatures. The Scherrer equation (2) is commonly used to calculate nanoscale crystallite size, and FWHM value is one of the two parameters determining the crystallite size. Bragg angle θ and FWHM are inversely proportional to crystallite size, while the variation of Bragg angle is small; thus, the crystallite size as seen in Figure 2(e) has the opposite trend with FWHM values.

$$D = \frac{K\lambda}{\beta \cos\theta}, \tag{2}$$

where D is the crystallite size (nm), K is a dimensionless shape factor, and β is FWHM.

Figure 4 shows the surface morphology of ZnO-H, AZO-H, and GZO-H films as-deposited and annealed at various temperatures. Generally, there is no significant difference in surface morphology between as-deposited films regardless of the appearance of aluminum or gallium and that annealed at 300°C or 500°C. Besides, based on SEM micrographs, it is clearly seen that the distribution of grain size for all films is homogenous on the surface and all films have the similar morphology, which indicates that films were well prepared and homogeneous.

The transmittance spectra of ZnO-H, AZO-H, and GZO-H thin films measured in wavelength range of 300–1100 nm in Figure 5 show clear and homogenous interference fringes of all films indicating the high crystalline quality and the similar film thickness, respectively. The inset in Figure 5(a) shows a red shift of all films with further increasing annealing temperature, because the decrease of n as seen in Figure 1(a) gives rise to the Burstein-Moss effect. The transmittance is larger than 82% (including film and glass substrate) when

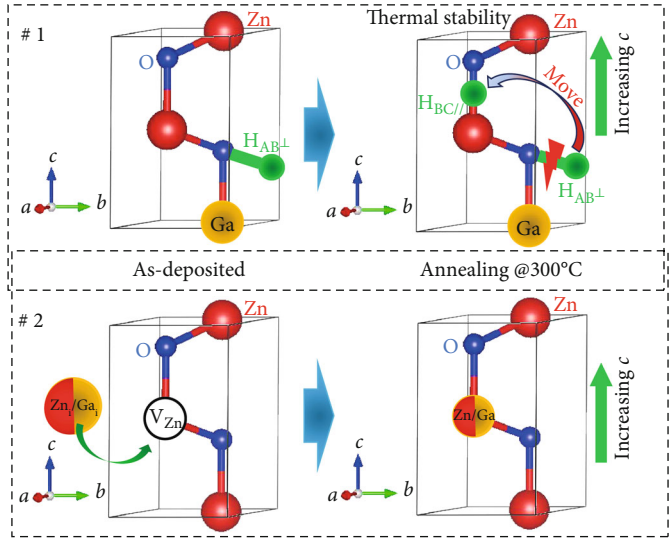

Figure 3: Illustrations of causes increasing lattice parameter *c* of ZnO-H and GZO-H films.

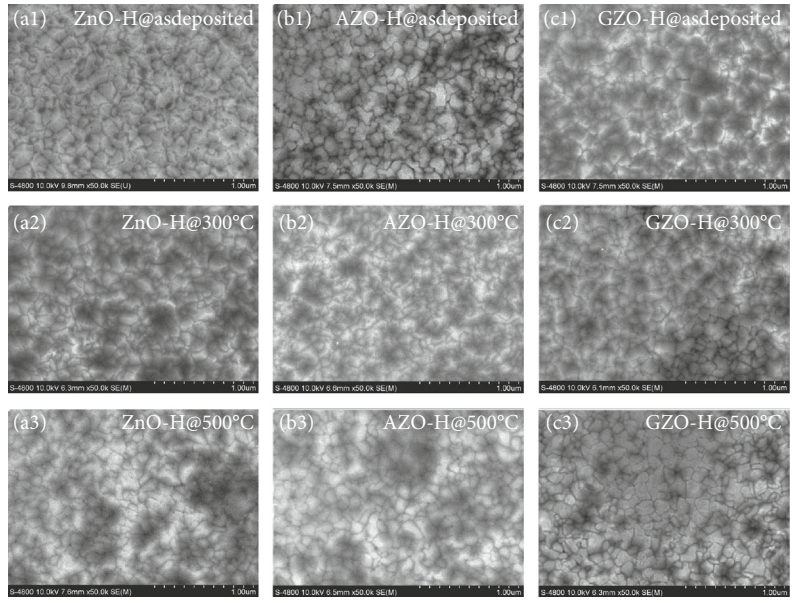

Figure 4: SEM micrographs of (a1–a3) ZnO-H, (b1–b3) AZO-H, and (c1–c3) GZO-H films prepared at different annealing temperatures.

averaged in the visible and near-infrared range from 400 to 1100 nm for all films as seen in Figure 5(b). The average transmittance of ZnO-H and AZO-H films has a decreasing trend when annealing temperature rises to 300°C. This is due to the formation of defects in host lattice generated from the broken hydrogen-related bonds as mentioned above, which gives rise to the appearance of scattering centers. However, the average transmittance of GZO-H films is almost unchanged at annealing temperature of 300°C, which is consistent with electrical properties as discussed above. With further increasing annealing temperature, the average transmittance of all films increases because of the aforementioned recrystallisation phenomenon.

Figure 6 shows the variation of the photoluminescence spectra of ZnO-H, AZO-H, and GZO-H thin films at different annealing temperatures. All films have a strong emission band in wavelength range of 375–450 nm, which is known as a featured emission band of ZnO material including near-band edge emission (NBE) [37, 38] and the transition between donor levels (such as Zn_i or H_i) and acceptor levels (V_{Zn}). The broaden emission band in wavelength range of 450–600 nm is attributed to the transition from oxygen vacancy levels to acceptor levels or valence band (VB) [37, 38]. From Figure 6, it can be clearly seen that there is a significant variation in shape of PL spectra of all films at different annealing temperatures, which indicates that annealing temperature strongly affects defect levels. In case of AZO-H films (Figure 6(b)), the PL intensity of AZO-H films significantly increases at annealing temperature of 300°C, which indicates that hydrogen is easy to cooperate with defects in AZO-H

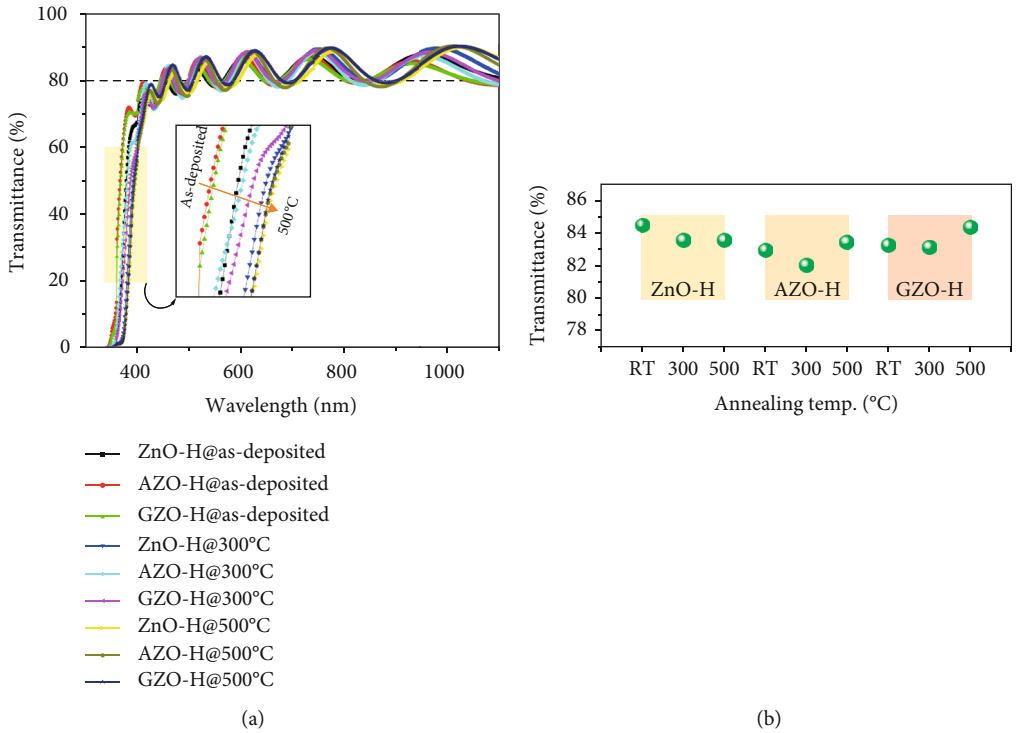

Figure 5: (a) Transmittance spectra of ZnO-H, AZO-H, and GZO-H at different annealing temperatures. (b) The dependence of the average transmittance of all films on annealing temperature.

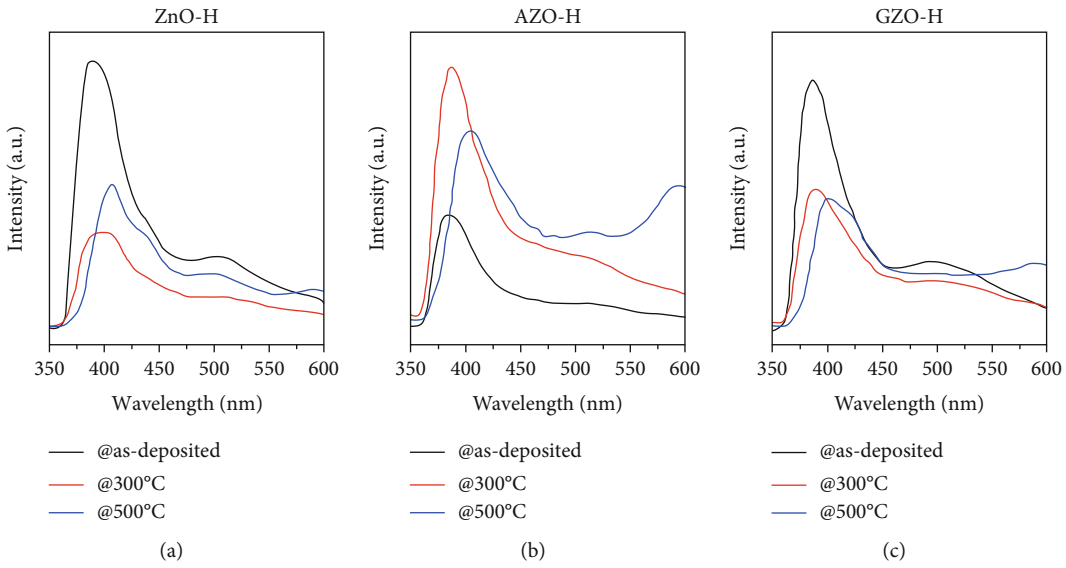

Figure 6: PL spectra of (a) ZnO-H, (b) AZO-H, and (c) GZO-H films annealed at different temperatures.

films such as H_i or V_{Zn} to effectively improve electron mobility and carrier concentration as seen in Figure 1, but these hydrogen-related bonds are easy to be broken, which results in defects. However, in the case of ZnO-H and GZO-H films, the defect-related emission has a slight variation. The intensity of all samples in wavelength range of around 600 nm strongly increases at annealing temperature of 500°C, which indicates that hydrogen diffused out of oxygen vacancy sites.

To get more details on the influence of annealing temperature on defects in ZnO-H, AZO-H, and GZO-H films, all PL spectra were deconvoluted based on Gaussian function distribution to determinate the overlapped emissions as seen in Figure 7. There are four deconvoluted emission peaks for all films. However, there is an absence or appearance of several PL peaks because of the annealing treatment. For example, for as-deposited and 300°C-annealed films (ZnO-H,

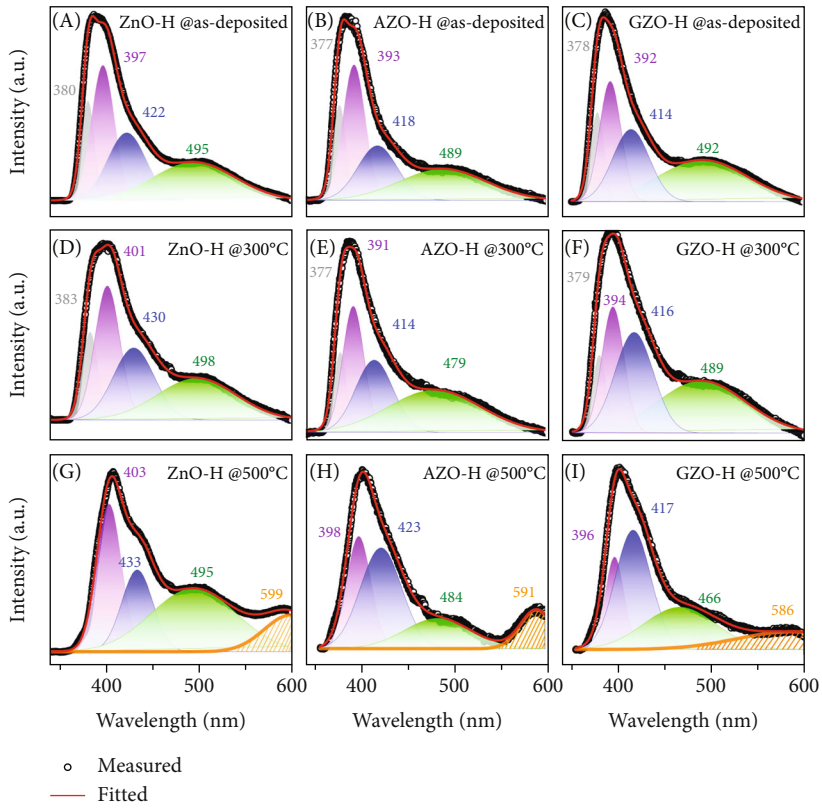

FIGURE 7: Deconvoluted photoluminescence spectra of (a, d, g) ZnO-H, (b, e, h) AZO-H, and (c, f, i) GZO-H films prepared at different annealing temperatures.

AZO-H, and GZO-H films), the emission peaks in the UV region (under 383 nm in this work) which is known as the transition of electrons between NBE states and VB were detected, while the yellow emission peak at around 600 nm which is attributed to the emission from conduction band (CB) to doubly charged oxygen vacancies ($V_O^{\bullet\bullet}$) appears in the films annealed at temperature of 500°C [4].

The violet region (391–403 nm) for all films (as-deposited and annealed films) is attributed to the transition from the Zn_i levels (located at 0.2 eV below the CB for a typical band-gap of 3.37 eV of ZnO) to VB or from CB to the V_{Zn} levels (located at 0.3 eV above VB) [39, 40]. For ZnO-H films, the violet emission peaks located in wavelength range of 397 nm (3.12 eV) to 403 nm (3.07 eV) are caused by the transitions from CB and NBE to V_{Zn} levels. However, for AZO-H and GZO-H films, the violet emissions fluctuate around the wavelength range of 391 nm (3.17 eV) to 398 nm (3.11 eV) which means that these emissions are well fitting with the transition of electrons from Zn_i levels to VB. The transition between Zn_i levels and VB prevails in AZO-H and GZO-H films in comparison with ZnO-H film because of the existence of Ga_i or Al_i which cannot completely substitute for Zn and behave as a shallow donor like Zn_i [41]. The near-blue emission peaks (414–433 nm and 2.99–2.86 eV, respectively) in PL spectra of ZnO-H, AZO-H, and GZO-H films (both as-deposited and annealed films) are the result of transition of electrons from Zn_i to V_{Zn} levels [3].

From the observation of the emissions in violet and near-blue regions in Figures 6 and 7, ZnO-H film has the larger red shift in comparison with GZO-H film because the broadness of V_{Zn} level relates to the broken V_{Zn}-H complexes at annealing temperature of 300°C. However, interestingly, AZO-H film has the blue shift in the violet and near-blue regions because of the narrowness of V_{Zn} levels which is caused by the formation of Al_{Zn}-V_{Zn} complex as proved by Johansen et al. [42]. The annealing temperature of 300°C is enough to break the V_{Zn}-H complex as well as gives rise to the combination of Al_{Zn} defect to the nearest V_{Zn} defect to form the Al_{Zn}-V_{Zn} complex. This complex limits the role of shallow Al_{Zn} donor because it acts as a compensating acceptor with the charge state of -1, which is consistent with the decrease of carrier concentration of AZO-H film annealed at temperature of 300°C as mentioned above.

The blue-green emission peaks (479–498 nm; 2.59–2.49 eV) are attributed to the transition of electrons from V_O^* defect (neutral oxygen vacancies formed by the $V_O^{\bullet}$ state captures an electron from CB) [3] or $V_O^{\bullet} - H$ complex to VB. Besides, the blue-green emission peaks of ZnO-H films have a red-shifted tendency, whereas those of AZO-H and GZO-H films have a blue-shifted tendency at annealing temperature of 300°C, which implies that there is an influence of Al or Ga on V_O-related defect level. From those PL results, we reveal that there is a small change in emission peaks of GZO-H films in comparison with ZnO-H and AZO-H films at

annealing temperature of 300°C, which indicates that GZO-H film is still stable at this annealing temperature and these PL results are consistent with electrical properties.

4. Conclusions

The influence of annealing temperature on electrical, optical, structural, and morphological properties of ZnO-H, AZO-H, and GZO-H films was systematically investigated to find out the thermal durability of those films. We reveal that GZO-H films are not only durable with respect to electrical properties at annealing temperature up to 300°C but also have slightly increased carrier concentration and electron mobility. Besides, we propose that Ga^{3+} ions located at adjacent Zn sites along with annealing temperature of 300°C can push hydrogen atoms into bond center sites forming $H_{BC//}$, which gives rise to the stability of electrical properties of GZO-H films. ZnO-H and AZO-H films have only thermal durability at annealing temperature up to 200°C.

Data Availability

The data that support the findings of this study are within the article and the raw data are available from the corresponding author, Vinh Cao Tran, upon reasonable request.

Conflicts of Interest

There are no conflicts of interest to declare.

Acknowledgments

This research is funded by Vietnam National University HoChiMinh City (VNU-HCM) under the grant number B2017-18-09. The Hall effect measurement was supported by the Faculty of Materials Science and Technology, University of Science, VNU-HCM.

Supplementary Materials

Graphical abstract depicting a model for briefly interpreting the thermal durability of GZO-H film can be found at the system on Journal of Nanomaterials. *(Supplementary Materials)*

References

[1] T. F. Wu, K. Zhao, B. W. Lü, Z. L. Wu, and Y. S. Wang, "Intrinsic defects in ZnO films deposited by RF sputtering," *Ferroelectrics*, vol. 528, no. 1, pp. 31–37, 2018.

[2] Y. J. Y. Onofre, S. de Castro, and M. P. F. de Godoy, "Effect of traps localization in ZnO thin films by photoluminescence spectroscopy," *Materials Letters*, vol. 188, pp. 37–40, 2017.

[3] F. Kayaci, S. Vempati, I. Donmez, N. Biyikli, and T. Uyar, "Role of zinc interstitials and oxygen vacancies of ZnO in photocatalysis: a bottom-up approach to control defect density," *Nanoscale*, vol. 6, no. 17, pp. 10224–10234, 2014.

[4] S. Ghose, T. Rakshit, R. Ranganathan, and D. Jana, "Role of Zn-interstitial defect states on d0 ferromagnetism of mechanically milled ZnO nanoparticles," *RSC Advances*, vol. 5, no. 121, pp. 99766–99774, 2015.

[5] B. Lin, Z. Fu, and Y. Jia, "Green luminescent center in undoped zinc oxide films deposited on silicon substrates," *Applied Physics Letters*, vol. 79, no. 7, pp. 943–945, 2001.

[6] G. Y. Huang, C. Y. Wang, and J. T. Wang, "First-principles study of diffusion of zinc vacancies and interstitials in ZnO," *Solid State Communications*, vol. 149, no. 5-6, pp. 199–204, 2009.

[7] C. G. Van De Walle, "Hydrogen as a cause of doping in zinc oxide," *Physical Review Letters*, vol. 85, no. 5, pp. 1012–1015, 2000.

[8] D. L. Zhu, G. J. Wang, F. Jia et al., "Study of H-related defects in Ga-doped ZnO thin films deposited by RF magnetron sputtering in Ar+H2 ambient," *Materials Technology*, vol. 32, no. 7, pp. 424–429, 2017.

[9] M. D. McCluskey and S. J. Jokela, "Defects in ZnO," *Journal of Applied Physics*, vol. 106, no. 7, article 071101, 2009.

[10] D. M. Hofmann, A. Hofstaetter, F. Leiter et al., "Hydrogen: a relevant shallow donor in zinc oxide," *Physical Review Letters*, vol. 88, no. 4, 2002.

[11] E. V. Lavrov, "Hydrogen in ZnO," *Physica B: Condensed Matter*, vol. 404, no. 23-24, pp. 5075–5079, 2009.

[12] J. Koßmann and C. Haettig, "Investigation of interstitial hydrogen and related defects in ZnO," *Physical Chemistry Chemical Physics*, vol. 14, no. 47, pp. 16392–16399, 2012.

[13] D. Gaspar, L. Pereira, K. Gehrke, B. Galler, E. Fortunato, and R. Martins, "High mobility hydrogenated zinc oxide thin films," *Solar Energy Materials and Solar Cells*, vol. 163, pp. 255–262, 2017.

[14] W. M. Kim, Y. H. Kim, J. S. Kim et al., "Hydrogen in polycrystalline ZnO thin films," *Journal of Physics D: Applied Physics*, vol. 43, no. 36, p. 365406, 2010.

[15] C. G. Van de Walle, "Hydrogen in semiconductors and insulators," *Journal of Alloys and Compounds*, vol. 446-447, pp. 48–51, 2007.

[16] M. G. Wardle, J. P. Goss, and P. R. Briddon, "First-principles study of the diffusion of hydrogen in ZnO," *Physical Review Letters*, vol. 96, no. 20, 2006.

[17] S. G. Koch, E. V. Lavrov, and J. Weber, "Interplay between interstitial and substitutional hydrogen donors in ZnO," *Physical Review B: Condensed Matter and Materials Physics*, vol. 89, no. 23, 2014.

[18] E. V. Lavrov, F. Börrnert, and J. Weber, "On the nature of hydrogen-related shallow donors in ZnO," *Physica B: Condensed Matter*, vol. 376-377, pp. 694–698, 2006.

[19] X. Li, B. Keyes, S. Asher et al., "Hydrogen passivation effect in nitrogen-doped ZnO thin films," *Applied Physics Letters*, vol. 86, no. 12, p. 122107, 2005.

[20] J. Bang and K. J. Chang, "Diffusion and thermal stability of hydrogen in ZnO," *Applied Physics Letters*, vol. 92, no. 13, p. 132109, 2008.

[21] J. Nomoto, H. Makino, and T. Yamamoto, "Carrier mobility of highly transparent conductive Al-doped ZnO polycrystalline films deposited by radio-frequency, direct-current, and radio-frequency-superimposed direct-current magnetron sputtering: Grain boundary effect and scattering in the grain bulk," *Journal of Applied Physics*, vol. 117, no. 4, p. 045304, 2015.

[22] J. Nomoto, H. Makino, and T. Yamamoto, "High-Hall-mobility Al-doped ZnO films having textured polycrystalline structure with a well-defined (0001) orientation," *Nanoscale Research Letters*, vol. 11, no. 1, p. 320, 2016.

[23] M. D. McCluskey, S. J. Jokela, and W. M. H. Oo, "Hydrogen donors in ZnO," *MRS Proceedings*, vol. 864, 2005.

[24] X. Xue, T. Wang, X. Jiang, J. Jiang, C. Pan, and Y. Wu, "Interaction of hydrogen with defects in ZnO nanoparticles – studied by positron annihilation, Raman and photoluminescence spectroscopy," *CrystEngComm*, vol. 16, no. 6, 2014.

[25] C. G. Van de Walle, "Hydrogen as a shallow center in semiconductors and oxides," *Physica Status Solidi B: Basic Research*, vol. 235, no. 1, pp. 89–95, 2003.

[26] M. D. McCluskey and S. J. Jokela, "Sources of n-type conductivity in ZnO," *Physica B: Condensed Matter*, vol. 401-402, pp. 355–357, 2007.

[27] Y. Hu, Y. Chen, J. Chen, X. Chen, and D. Ma, "Effects of hydrogen flow on properties of hydrogen doped ZnO thin films prepared by RF magnetron sputtering," *Applied Physics A*, vol. 114, pp. 875–882, 2014.

[28] M. D. Mccluskey and S. J. Jokela, "Infrared spectroscopy of hydrogen in ZnO," *MRS Proceedings*, vol. 813, 2004.

[29] J. Cho, K.-H. Yoon, M.-S. Oh, and W.-K. Choi, "Effects of H[sub 2] annealing treatment on photoluminescence and structure of ZnO:Al/Al[sub 2]O[sub 3] grown by radio-frequency magnetron sputtering," *Journal of the Electrochemical Society*, vol. 150, no. 10, p. H225, 2003.

[30] D. L. Zhu, H. F. Xiang, P. J. Cao et al., "Influence of H2 introduction on properties in Al-doped ZnO thin films prepared by RF magnetron sputtering at room temperature," *Journal of Materials Science: Materials in Electronics*, vol. 24, no. 6, pp. 1966–1969, 2013.

[31] B. L. Zhu, J. Wang, S. J. Zhu et al., "Influence of hydrogen introduction on structure and properties of ZnO thin films during sputtering and post-annealing," *Thin Solid Films*, vol. 519, no. 11, pp. 3809–3815, 2011.

[32] M. D. McCluskey, M. C. Tarun, and S. T. Teklemichael, "Hydrogen in oxide semiconductors," *Journal of Materials Research*, vol. 27, no. 17, pp. 2190–2198, 2012.

[33] M.-C. Chen, T.-C. Chang, S.-Y. Huang et al., "A low-temperature method for improving the performance of sputter-deposited ZnO thin-film transistors with supercritical fluid," *Applied Physics Letters*, vol. 94, no. 16, p. 162111, 2009.

[34] F. T. Kong, H. J. Tao, and H. R. Gong, "Interstitial hydrogen in ZnO and BeZnO," *International Journal of Hydrogen Energy*, vol. 38, no. 14, pp. 5974–5982, 2013.

[35] M.-C. Li, C.-C. Kuo, S.-H. Peng, S.-H. Chen, and C.-C. Lee, "Influence of hydrogen on the properties of Al and Ga-doped ZnO films at room temperature," *Applied Optics*, vol. 50, no. 9, pp. C197–C200, 2011.

[36] D. P. Pham, H. T. Nguyen, B. T. Phan, V. D. Hoang, S. Maenosono, and C. V. Tran, "Influence of addition of indium and of post-annealing on structural, electrical and optical properties of gallium-doped zinc oxide thin films deposited by direct-current magnetron sputtering," *Thin Solid Films*, vol. 583, pp. 201–204, 2015.

[37] A. Tiwari and P. P. Sahay, "The effects of Sn-In co-doping on the structural, optical, photoluminescence and electrical characteristics of the sol-gel processed ZnO thin films," *Optical Materials*, vol. 110, p. 110395, 2020.

[38] X. Chen, Q. Xie, and J. Li, "Significantly improved photoluminescence properties of ZnO thin films by lithium doping," *Ceramics International*, vol. 46, no. 2, pp. 2309–2316, 2020.

[39] Y. M. Hu, J. Y. Li, N. Y. Chen, C. Y. Chen, T. C. Han, and C. C. Yu, "Effect of sputtering power on crystallinity, intrinsic defects, and optical and electrical properties of Al-doped ZnO transparent conducting thin films for optoelectronic devices," *Journal of Applied Physics*, vol. 121, no. 8, p. 085302, 2017.

[40] C. H. Ahn, Y. Y. Kim, D. C. Kim, S. K. Mohanta, and H. K. Cho, "A comparative analysis of deep level emission in ZnO layers deposited by various methods," *Journal of Applied Physics*, vol. 105, no. 1, p. 013502, 2009.

[41] A. Janotti and C. G. Van de Walle, "Fundamentals of zinc oxide as a semiconductor," *Reports on Progress in Physics*, vol. 72, no. 12, p. 126501, 2009.

[42] K. M. Johansen, L. Vines, T. S. Bjørheim, R. Schifano, and B. G. Svensson, "Aluminum migration and intrinsic defect interaction in single-crystal zinc oxide," *Physical Review Applied*, vol. 3, no. 2, 2015.